Technical Report No. 32-635

A Momentum-Balance Method for Measuring the Thickness of Free Liquid Sheets

George I. Jaivin

jpl

JET PROPULSION LABORATORY
CALIFORNIA INSTITUTE OF TECHNOLOGY
PASADENA, CALIFORNIA

August 17, 1964

Technical Report No. 32-635

A Momentum-Balance Method for Measuring the Thickness of Free Liquid Sheets

George I. Jaivin

D. R. Bartz, Chief
Propulsion Research Section

JET PROPULSION LABORATORY
CALIFORNIA INSTITUTE OF TECHNOLOGY
PASADENA, CALIFORNIA

August 17, 1964

CONTENTS

FIGURES

ABSTRACT

A method is presented for determining experimentally the momentum-averaged thickness of free liquid sheets. The technique requires the experimental determination of the reaction force produced by a sector of a liquid sheet upon a deflection plate placed in its path. This measurement, together with a weight flow rate, is used to calculate the local thickness and average velocity of the sheet by simultaneous solution of the applicable momentum and flow continuity relations. Details of the experimental apparatus are presented, and the results obtained when the apparatus was used to evaluate an axially symmetric laminar liquid sheet are given.

I. INTRODUCTION

A. Background

A study of the processes involved in the atomization of liquids has occupied the attention of many investigators for a considerable period of time. The continuing effort to understand the significant factors underlying the processes involved in the disintegration of fluid sheets and jets is stimulated by the potential value such information may yield in many diverse areas of engineering endeavor. Typical examples of such applications include the drying and liquid-spray-cooling techniques employed in chemical engineering processes, the diesel injection devices used widely in the automotive field, and the propellant-injection schemes used both for turbojet and rocket-engine applications.

At the Jet Propulsion Laboratory, primary emphasis in this area has been placed on an attempt to evaluate the significant parameters affecting the breakup of liquid sheets and, ultimately, to correlate these with the droplet size distribution in the resultant spray. It should be recognized that most of the schemes employed for injecting propellants into a rocket-engine chamber depend, at least in part, on the disintegration of a liquid sheet for the atomization and dispersion of the propellants, and hence, the data generated in this investigation should produce information applicable to a broad spectrum of injection devices currently being used. The doublet injection configuration, for example, which is widely used in rocket-engine injector designs today (i.e., one jet of propellant impinging on another jet of propellant, whether like-on-like or like-on-unlike), will typically produce a liquid sheet; this, in turn, breaks up to form a dispersed spray of the injectants. Other types of injectors involving jet impingement, such as triplets, etc., display similar spray-evolution characteristics. In

addition, conventional spray nozzles, such as swirl atomizers, characteristically produce a hollow, conical liquid sheet as an initial step in the atomization process. Thus, it is apparent that an understanding of the atomization of liquid sheets will provide the data necessary to supply the missing link in the chain of events which finally result in the formation of a spray.

B. The Problem

The term, free jet, refers in the general sense to fluid in motion that is bounded by a surface of constant pressure. This surface may also be associated with a discontinuity such as exists with a liquid jet in air, where a step change in fluid density occurs; but it is still true that if extraneous forces are neglected, the pressure must be constant along such a surface (Ref. 1). It should be recognized that the free liquid sheet readily falls within the bounds of the above definition and is, in reality, a particular type of free jet. It is a characteristic of a free liquid sheet that its thickness is considerably less than its length or width. The surface of the sheet may be either flat or curved. Throughout this Report, the term, free liquid sheet, shall be further restricted to include only those flows which characteristically exhibit the propensity to generate new or additional surface area; additionally, it is noted that such a flow configuration would, as a consequence of the above considerations, display a spatial variation in the thickness of the sheet. Specifically excluded by the above restraints are, for example, flows such as one would observe from a long, narrow slit supplied with liquid from a large, upstream reservoir, i.e., a two-dimensional jet. While its initial appearance would be sheet-like, the flow from such a source would display none of the intrinsically unstable features of a free sheet but would instead, under the influence of surface tension, tend toward a cylindrical jet configuration.

The basic principle involved in the breakup of a liquid sheet consists of increasing the surface of the sheet until it ultimately becomes unstable and disintegrates. The stability of a sheet may be defined as its resistance to disintegration. Hence, the most stable sheet would tend to be least affected by flow turbulence and air resistance and would have its region of disintegration farthest from the sheet source. When two cylindrical jets of liquid flowing at a low jet Reynolds number are made to impinge upon each other from two opposed orifices having a common centerline, an axially symmetric liquid sheet is produced. Hypothetically, if the flow is free of all disturbances, both internal and external, and if the effects

of gravity are neglected, the sheet will grow increasingly larger and thinner. Since energy must be supplied to generate new sheet surface, ultimately, the total kinetic energy of the flow is converted to potential energy stored in the sheet surface. When this point is reached, the edge of the sheet experiences an unbalanced force as a result of the undiminished surface tension acting on the rim of the sheet, and the edge begins to contract. A stable equilibrium position for the circular rim of the sheet is established where the surface tension (or contraction) force equals the inertia (or expansion) force produced by the fluid entering and being decelerated by the fluid already in the rim. This equilibrium model is patterned after an analysis by Ranz (Ref. 2), except that, in this case, the fluid moves into a stationary rim; the converse situation was studied by Ranz. Any disturbance superimposed upon the equilibrium of the two forces will lead to earlier disruption of the sheet. When this takes place, the inertia force becomes greater than that of surface tension, and drops are formed at the leading edge which leave the rim as liquid threads or filaments. The filaments, in turn, become unstable and break up into droplets.

As the velocity of the sheet is increased, the interaction between the rapidly moving surface of the sheet and the relatively quiescent surroundings becomes increasingly evident. Initially, the aerodynamic forces cause waves to be built up in the sheet near the region of disintegration. (A detailed description of this phenomenon is given in Ref. 3.) The initial disturbance triggering the formation of the waves may be a result of either the turbulence in the sheet or the air entrained by the sheet. With a further increase in the velocity, the disturbance caused by the waves becomes more pronounced, and the region of disintegration begins to recede toward the center of the sheet. The spatial mass distribution of the resulting spray is increased by the dispersion caused by the wavy sheet surface. Further increases in the velocity result in sheet breakup in the immediate vicinity of the sheet source.

An increased level of turbulence usually accompanies an increased flow velocity. The effect of the higher turbulence level is reflected in the onset of a ruffled sheet surface as well as a decrease in the length of the sheet prior to breakup. Perforations or holes appear spontaneously in the sheet surface and, in some instances, are the major factor inducing the disintegration of the sheet. Often, both the surface waves produced by aerodynamic interaction and the holes in the sheet are seen.

While other factors, such as droplets striking the surface, may be of some importance in explaining the origin of the holes, they are most probably the result of highly disturbed local areas in the sheet. Observations made of turbulent sheets have shown an apparent increase in the incidence of holes with increasing turbulence levels, which then leads to significantly earlier breakup of the sheets (Ref. 4).

Thus, one reaches the *a posteriori* conclusion that turbulence and air resistance are two of the dominant parameters controlling the disintegration process. Intuitively, it can be reasoned that other factors may also be of importance. The apparent disruptive influence of non-uniform velocity profiles upon certain free liquid jets as noted by Rupe (Ref. 1) may also be significant in the breakup of sheets of liquid. Fluid properties, such as surface tension and viscosity, have also been shown to be important parameters affecting the stability of liquid sheets (e.g., Ref. 5).

The brief physiographical description of the breakup of a liquid sheet given above only serves to point up the complexity of the physical processes taking place in the sheet. In order to fully understand the mechanisms controlling the disintegration of a liquid sheet, it is imperative that a detailed accounting be made of the significant parameters characterizing the phenomena. While the physical characteristics of the liquid, such as surface tension, density, and viscosity, can be easily ascertained, the hydrodynamic properties of the flow system are not so readily determined. Of interest, for example, are local measurements of average sheet velocity, thickness, turbulence level, and velocity profile through the sheet cross-section. In addition, data on both the length of the free sheet prior to breakup and the resulting droplet size distribution are considered important factors in describing the disintegration processes. Pertinent experimental data are needed to evaluate the relative significance of these parameters and, ultimately, to allow a more complete description of the atomization processes to be made.

Measurement of the local thickness in a liquid sheet would be significant for several reasons. This information, along with prior local flow-rate data, is sufficient to make possible an estimate of the local average velocity by use of the mass conservation relationship (see Section D, for example). In addition, it is believed that information regarding the sheet thickness at the breakup region may be important for the eventual correlation of this property with the resulting droplet size distribution.

The experimental problems attendant to such an investigation of sheet thickness arise partly because of the inherent complexities of the flow being studied. The impingement of two cylindrical liquid jets, one upon the other, offers a greater degree of simplicity and control over the hydrodynamic properties than most of the other means available for forming a liquid sheet. Moreover, if two identical opposed jets are used, the resultant sheet is flat and axially symmetric, thus greatly simplifying the geometry of the entire flow system. The symmetrical dispersion of the liquid from the impingement point readily permits accurate estimates to be made of the local radial flow rates. A flow fixture which produced a free liquid sheet having these desirable features was utilized for the series of experiments described in this Report.

The dynamic properties of a symmetric sheet are difficult to measure, as many of these parameters are continuously varying throughout the sheet. Because of practical limitations imposed by weight flow, the thicknesses of the symmetrical sheets that were studied are nominally quite small, being in the neighborhood of several hundredths of an inch near their source and rapidly decreasing with increasing radius. Hence, any device to be employed for the direct measurement of the sheet thickness must, of necessity, be reasonably small in order to reduce the disturbances introduced as a result of its use. Nevertheless, insertion of any object into the sheet invariably disrupts it at that point regardless of the size of the apparatus, thus necessitating the use of appropriate correction factors to account for such a disturbance. The alternate approach of employing devices designed to be used externally, such as optical instruments, is also hampered because the sheet surface is not flat everywhere. As discussed earlier, the surface of the sheet, even under near-ideal conditions, is wavelike, with the wave amplitude increasing as a function of radius.

The purpose of this Report is the exposition of the pertinent details relevant to the design, fabrication, and operation of a probe suitable for measuring the momentum of a sector of an axially symmetric liquid sheet. These empirically determined momentum data, together with appropriate local weight flow measurements, are sufficient to permit a calculation of the local thickness of the sheet to be made. Details of the experimental apparatus and procedures are presented, as well as a discussion of the theory and the significance of the observed results.

C. Review of Literature

Many different approaches to the problem of the determination of sheet thickness have been attempted. Most of these have involved indirect or inferential methods of measurement. An exception was the work of Dombrowski and Fraser (Ref. 5), who directly measured the volume flow rate of liquid passing through a small, intercepted sector of the sheet. This information, along with an assumed sheet velocity, can be used to compute the sheet thickness. Apart from the obvious difficulty of accurately estimating the local velocity in the sheet, this technique is appealing because of its apparent simplicity.

Dixon, et al. (Ref. 6) measured the light absorption through dyed sheets of liquid and correlated their readings with calibrated color density standards to determine the thickness. Variations in sheet thickness corresponding to waves in the sheet were noted, but no further work was done to substantiate these findings. It is felt that the observed results may be a consequence of the differences in the transmitted light intensity caused by variations in the reflective properties of the wavy surface of the sheet. Taking advantage of the reflection characteristics of thin films, Dombrowski, et al. (Ref. 7) developed a technique utilizing light interferometry, which, with smooth sheets, permitted a complete thickness survey to be made at one time. Oblique illumination of the sheet with monochromatic light formed an interference pattern of light and dark stripes which could then be photographed. After establishing a reference thickness corresponding to a specific dark band, the thickness throughout the sheet could be determined simply by counting interference fringes. The obvious drawback is the necessity of producing sheets having the prerequisite smooth surface. The measurements that were reported were made of small, laminar, relatively low-velocity fan-type sheets. The experimental procedure is unsuitable for moderate- or high-velocity sheets, or those with turbulence, because the surfaces of such sheets are invariably ruffled or wavy. Such surfaces produce distorted interference patterns which are usually impossible to interpret properly.

Dukler and Bergelin (Ref. 8) measured the capacitance changes produced by a sheet of liquid flowing between two parallel metal plates, which were connected electrically to form a condenser. In their experimental apparatus, the liquid flowed down a fixed vertical flat plate, and a second movable plate serving as a probe was positioned adjacent to the fixed plate. The flowing liquid on the plate acted as a variable-thickness dielec-

tric material, and the resulting variation in capacitance was recorded and related to the film thickness by an appropriate calibration scheme. The sensitivity of devices of this kind depends partly on the spacing between the surfaces serving as the capacitor elements. In order to use such an arrangement for monitoring the thickness of a free liquid sheet, relatively wide spacing of the sensing elements would be required to prevent the wavy surface of the sheet from impinging upon them. This spacing would greatly reduce the sensitivity of the apparatus and thus would probably make it unsuitable for such an application.

Berthold (Ref. 9) holds a patent on a device for measuring the thickness of thin films of various materials by measuring the attenuation of beta-rays passed through them. It is claimed that by employing a high-energy beta-ray source and a null-balance potentiometer detection scheme, improved accuracy is achieved over a broad thickness range. No mention is made of its possible use for the measurement of liquid film thicknesses, but such an application might prove fruitful if adequate resolution and reproducibility could be obtained.

Wilkes and Nedderman (Ref. 10) employed a method involving stereophotography of small particles or bubbles in thin liquid films. By use of multiple photographic exposures and modified stereoscopic mapping equipment, they were able to determine velocities in thin films adjacent to fixed boundaries. While they have restricted their work to date to studies of velocity distributions, it appears that a logical extension of their effort could include thickness determinations. Since the method involves the tracking of particles, it is not suited to the study of very thin sheets because of the disruptive influence such particles would have upon the sheets. In addition, because of optical constraints, such as the very limited depth of field of the instrument, the scheme would have limited application when used with free liquid sheets having nonsteady spatial boundaries.

Lukens (Ref. 11) has studied the long-term luminescence of certain fluids after excitation by ultraviolet irradiation and has used this phenomenon to determine the thickness of liquid films by measuring the emitted light with a photomultiplier tube. The thin films were formed on the bottom of small, opaque cups and were examined by inserting the light-sensing device into the cup after exposing the sample to an ultraviolet source. Since the emitted light was quite feeble, precautions such as these must be taken to prevent extraneous light from reaching the sensor. Such a procedure, if

applied to a flowing liquid system, would require similar precautionary measures.

D. Momentum Probe Concept

The *impulse–momentum* theorem of mechanics, readily derivable from Newton's second law of motion, states that the product of a force and the increment of time during which it acts (i.e., the impulse of the force) equal the resulting change in the product of the mass of the

body on which the force acts and the velocity of the body (i.e., the change in the momentum of the body). Both impulse and momentum are necessarily vector quantities. It follows from the laws of motion that a mass cannot undergo a change of momentum except by application of an external force. The foregoing theorem is readily applied to problems dealing with flowing fluids. In such problems, the mass considered may be the mass discharged in any convenient time *t*. By means of this substitution, an equivalent expression applicable to
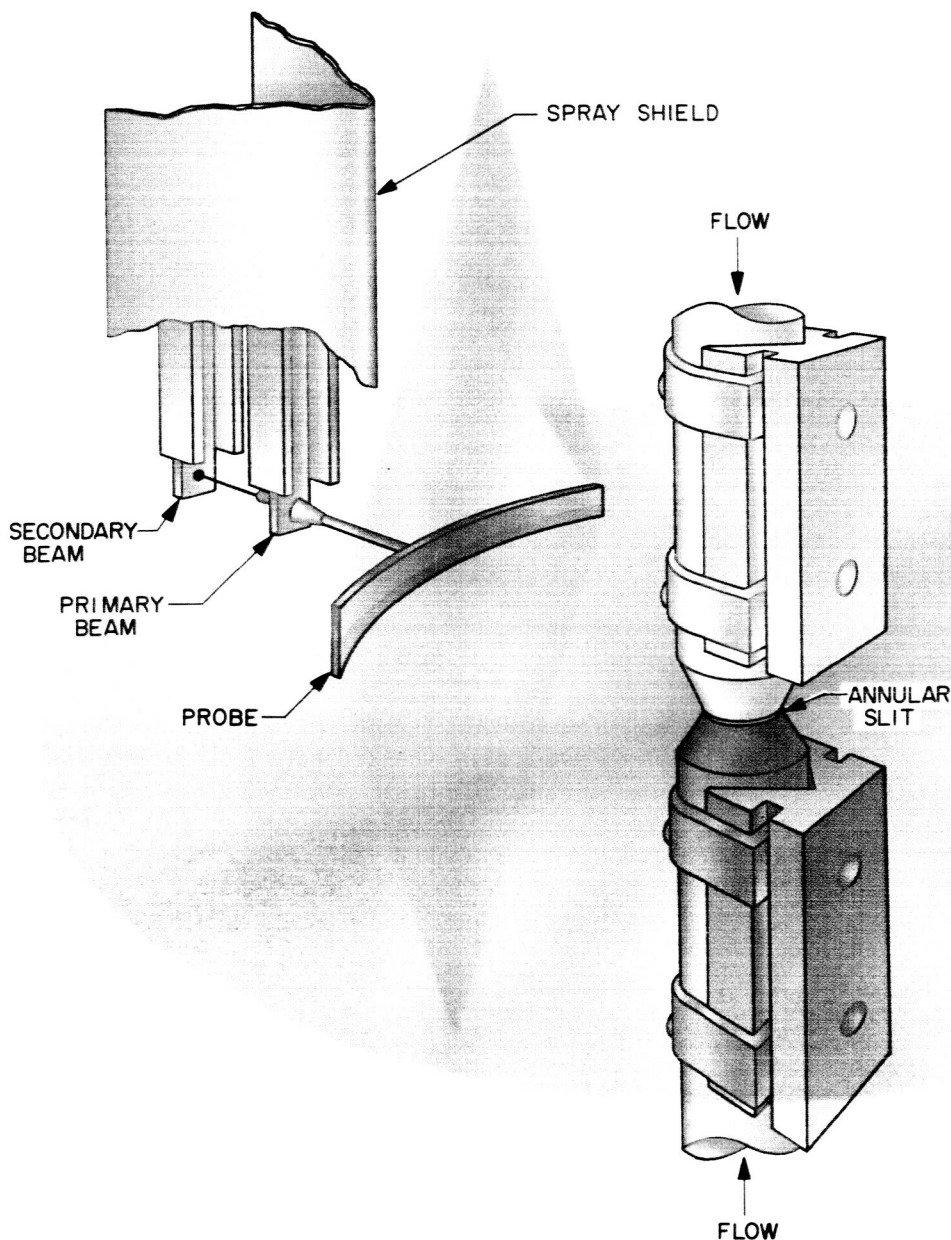

Fig. 1. Sketch of momentum-balance system in operation

fluids in motion is obtained. It may be stated as follows: The force exerted on the flow obstruction by a moving stream of fluid is equal to the time rate of change of momentum of the stream produced by the obstruction. This statement is a generally valid expression of the conservation of momentum principle as applied to a flowing fluid system. Its application to the problem of the measurement of the thickness of a liquid sheet is outlined below.

The flow in an axially symmetric liquid sheet can be assumed to be radial. Moreover, symmetry requires the flow rate per unit angle to be a constant. These conditions are not unrealistically difficult to achieve in a well designed flow system. Whereas the total integrated net momentum of an axially symmetric liquid sheet having a planar resultant is zero, the momentum of a sector of such a sheet is obviously not zero. In order to measure the momentum of a sheet sector, it was made to impinge upon a flat plate inserted in the flow, which, in the plane of the sheet, had a constant radius of curvature relative to the flow source (see Fig. 1). The flow striking the plate was turned through an angle of 90 deg, such that it left the surface of the plate normal to its original direction of motion. Therefore, the reaction force exerted on the plate in order to keep it in place could immediately be equated to the momentum of the flow impinging on it. Note that the radial flow impinging on the curved plate will strike the plate normally everywhere. Since only one component of the total force imparted to the deflection plate would be measured by a uniaxial thrust-measuring system, an appropriate correction must be made to the data to account for this factor.

In the following analysis, the effects of gravity have been excluded. Consider the sketch shown in Fig. 2. At point P, the velocity vector V is directed normal to the surface of the plate as it is everywhere else on the deflector. The velocity component parallel to the sector bisector (the X-direction) is $V \cos \theta$. The differential weight flow at P corresponding to the velocity V is given by $\dot{w}d\theta/2\pi$, and hence, the differential momentum in the X-direction at P is $\dot{w}V \cos \theta \ d\theta/2\pi g$. Integrating over the entire 60-deg sector of the plate yields the reaction force F; namely,

$$F = \int_{-\frac{\pi}{6}}^{\frac{\pi}{6}} \frac{\dot{w}V \cos \theta \ d\theta}{2\pi g} = \frac{\dot{w}V}{2\pi g} \qquad (1)$$

The average velocity of the sheet V is therefore seen to be

$$V = \frac{2\pi Fg}{\dot{w}} \qquad (2)$$

If the flow throughout the sheet is radial, conservation of mass can be expressed as $\dot{w} = \rho V 2\pi r t$, or, solving for t,

$$t = \frac{\dot{w}}{2\pi r \rho V} \qquad (3)$$

Substituting V from Eq. (2) into Eq. (3) finally yields

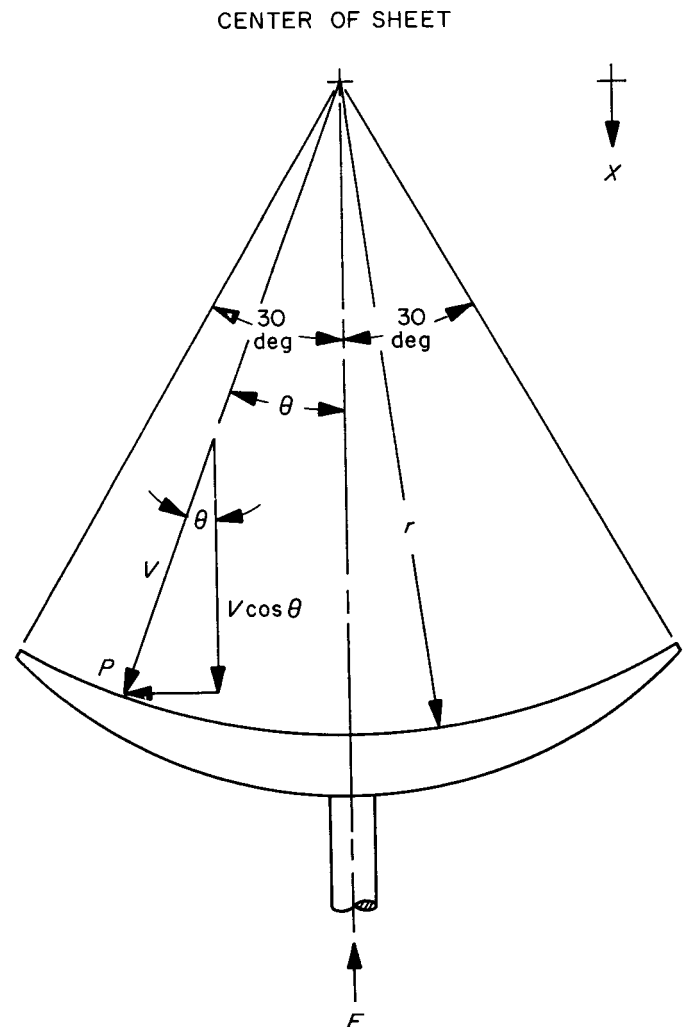$$t = \frac{\dot{w}^2}{4\pi^2 r \rho F g} \qquad (4)$$

Fig. 2. Pertinent geometry of deflection plate

Hence, from experimental measurements of $\dot{w}$ and F, both the momentum averaged local thickness and average velocity of the sheet can be determined from Eqs. (4) and (2), respectively. It should be noted that the velocity is averaged on the basis of the momentum measurement and is not necessarily the same value one would obtain from a weight flow average, for example.

Nevertheless, it is a valid representation of this particular parameter. The momentum measurement is an averaging technique and presupposes symmetric and angularly invariant flow conditions throughout the sheet. Therefore, it is applicable only to sheets incorporating those features or to those whose specific local flow rates and directions are known.

II. EXPERIMENTAL METHODS AND APPARATUS

A. Functional Description of Equipment

The momentum probe essentially consists of a device for experimentally measuring the thrust, or reaction force, produced by the change in momentum of the flow impinging upon a deflector inserted into a portion of a free liquid sheet. In order for meaningful data to be obtained by the employment of such a scheme, certain criteria must be satisfied:

1. The flow intercepted by the deflector must be turned through a known angle, preferably 90 deg.

2. The deflector must be so constructed that similar flow conditions prevail over its effective surface area.

3. Accurate and reproducible positioning of the deflector must be achieved when it is placed in the flow.

4. Accurate and reproducible measurements of the reaction force on the deflector must be obtained.

In general, it is observed that in order for flow, impinging normally upon an obstruction such as a flat plate, to be turned through a 90-deg angle, it is necessary for the plate to appear, to the flow, to be essentially infinite in extent. The actual physical dimensions required are a function of the pertinent scale of the flow system in every instance. In order to satisfy criterion 1 stated above, it was found that, for the flow configuration evaluated here, a ⅜-in.-wide deflector was adequate to cause the impinging sheet to be fully diverted.

The maximum thickness of the sheet, corresponding to the point of measurement closest to the flow source, was on the order of a few thousandths of an inch.

Since an axially symmetric sheet was used, the hydrodynamic conditions which existed at all points equidistant from the apparent line flow source had to be the same. Therefore, the surface of the deflector was curved such that all points on it were equidistant from the line source, thus meeting the requirements of criterion 2 as long as the deflector was properly positioned in the sheet.

The deflector plate, designed to intercept and divert a 60-deg sector of the sheet at a specific radial location, was mounted on a strain-gage-instrumented cantilever beam, called the primary beam, which served to position the deflector in the sheet. Connected to the primary beam by means of a pivot pin system was a secondary strain-gage-instrumented cantilever beam. Both of these beams were mounted on a traversing mechanism which permitted each to be independently positioned. The complete assembly is shown in Fig. 3. The electrical outputs of the two beams were noted after the deflector was properly positioned relative to the axis of the sheet. When the flow was initiated, the force generated on the deflector moved both beams away from their original positions. The deflector was restored to its original location in the flow by moving the secondary beam relative to the primary beam until the electrical output from the primary beam was the same as that previously recorded. The difference in the output from the strain gages
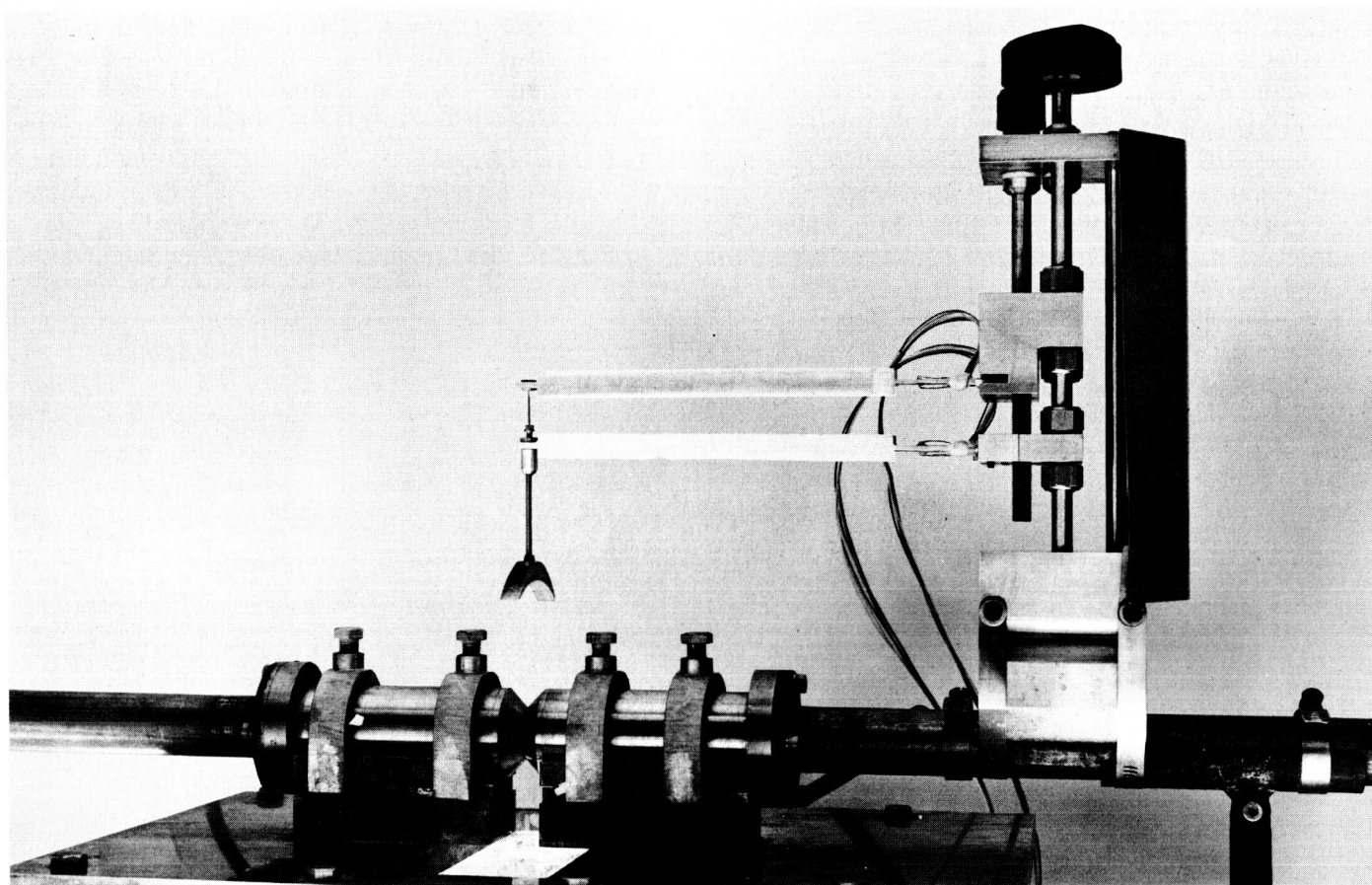
Fig. 3. Momentum-balance system assembly attached to sheet fixture

mounted on the secondary beam could then be correlated with the force exerted on the deflector by means of a suitable calibration factor. Thus, the use of two interconnected beam assemblies served the dual functions of positioning the deflector plate and measuring the thrust exerted on it.

B. Details of Constituent Parts

1. Deflection Plates

Seven deflection plates were built, each designed to intercept a 60-deg sector of the sheet at a specific radial distance from the flow centerline. The radii of curvature of these plates were 1.75, 2.00, 2.50, 3.00, 3.50, 4.00, and 4.50 in. (see Fig. 4). The width of the impingement surface of each deflector was ⅜ in. As discussed earlier, this width was chosen to ensure the complete turning of the flow striking the plate. In an attempt to determine the angle at which the flow actually left the surface of the plate, an eight-power telescope fitted with a calibrated reticle was used. It was found that the variance of the exit angle from the assumed 90 deg was negligible over the range of flow velocities studied.

The probes were machined to eliminate excess material and were fabricated from magnesium in order to keep their weight to a minimum. The deflector configuration designated as Type 1 in Fig. 4 corresponds to the plates having the five largest radii of curvature, while the Type 2 configuration was used for the other two deflector plates. The impingement surface of each deflection plate was lapped as a final machining operation to provide a smooth surface, and the edges were kept sharp and burr-free to prevent untoward flow separation effects from invalidating the data. Each probe had provision on the back surface for attaching it to the supporting rod which connected it to the primary beam. The attachment was in the form of a ball-and-socket arrangement to simplify the alignment procedure.

2. Thrust Beams

Both the position of the deflector and the thrust exerted on it by the impinging flow were measured using strain-gage-instrumented cantilever beams. The beams were designed to be extremely rigid along most of their length, except for a thin section adjacent to the clamped end of the beam (Fig. 5) to minimize the deflection at the free end produced by the application of a load. Two strain gages were attached on each side of the beam at the thin working section and were electrically connected to form a wheatstone bridge having four active arms. The beams were made of aluminum, and the gages used were appropriately temperature-compensated for that material.

In order to maximize the resolution of the device, five beams of varying load capacities were built for use as the secondary beam. As the force to be measured was increased, beams having greater rigidity were used to prevent overstressing of the material and to avoid excessive deflections at the free end of the beams (see listing in Fig. 5). In all cases, the primary beam had a 0.020-in. working section to obtain high resolution for accurate repositioning of the deflector.

The interconnection of the beams was accomplished by use of a pivot pin arrangement. Conical sockets were mounted on the back side of the primary beam and on the front side of the secondary beam. A steel pin, sharpened to a point at both ends, was inserted between the sockets on the beams and was aligned to coincide with the direction of the thrust vector. In this way, a minimum-friction pivot was provided, which allowed the two beams to move under load without imposing bending moments at the free ends.

3. Traversing Mechanism

The two beams were mounted on a traversing mechanism which permitted each beam to be positioned independently. This facilitated the proper alignment of the primary beam and made possible the relative motion between the beams needed to restore the deflector to its original location when a force was applied to the system.

The apparatus (Fig. 6) consisted of two rigidly supported parallel rods on which two movable slider-block assemblies were mounted. Each slider block, serving as the clamping fixture for one of the beams, was driven along the support rods by a precision-ground lead screw
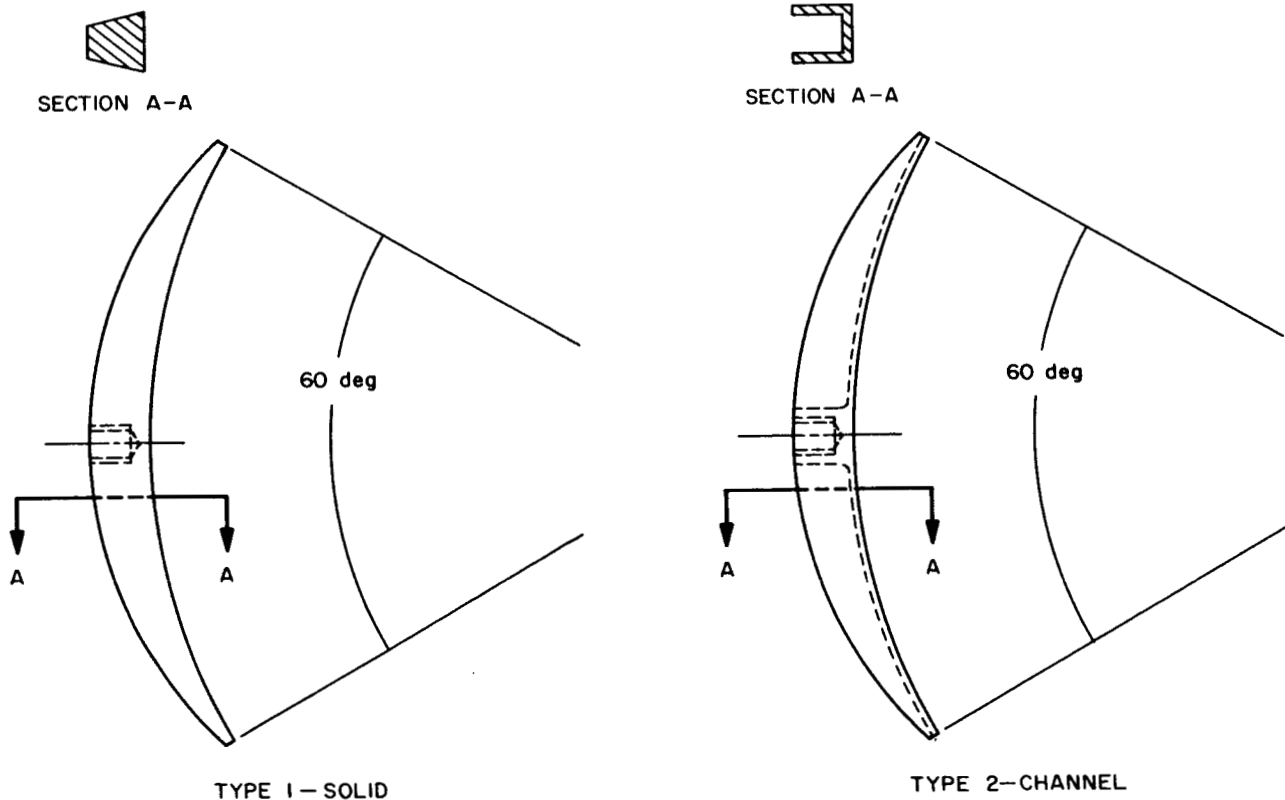

SECTION A-A

TYPE I — SOLID

SECTION A-A

TYPE 2—CHANNEL

Fig. 4. Details of deflection plates

SECTION A-A

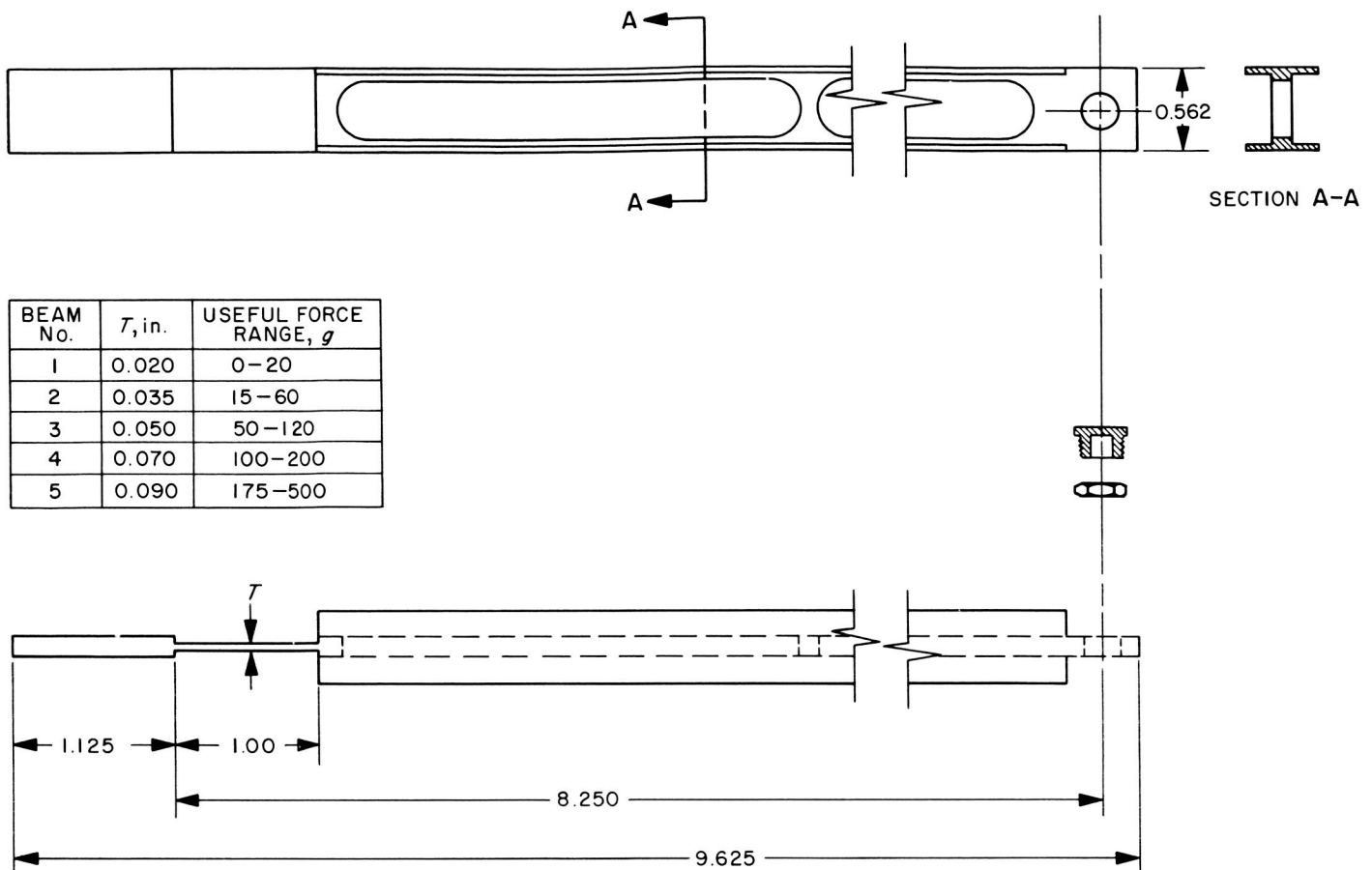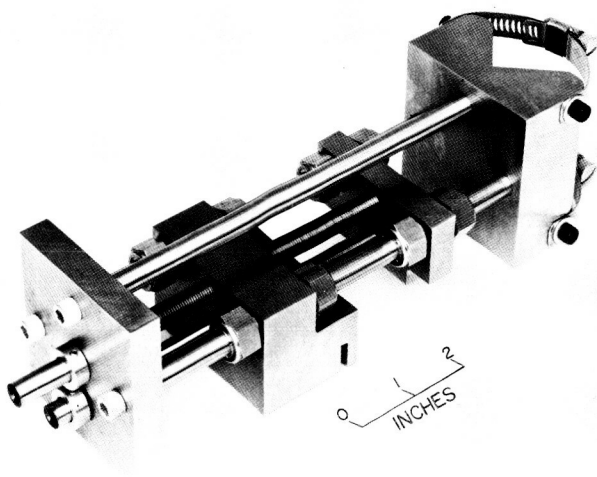| BEAM No.	T, in.	USEFUL FORCE RANGE, g
1	0.020	0 – 20
2	0.035	15 – 60
3	0.050	50 – 120
4	0.070	100 – 200
5	0.090	175 – 500

Fig. 5. Details of thrust beams

Fig. 6. Traversing-mechanism assembly

to ensure uniform motion of the block. The entire assembly was rigidly clamped to the sheet fixture in a manner which allowed the beams to be moved in a radial direction. A shield consisting of several pieces of thin stainless-steel plate was also mounted on the traverse to protect the beam assembly and strain gages from the spray generated by the deflector plate. Although waterproofing materials, such as silicon grease, were applied to the strain gages, it was found that the auxiliary shielding of the gages was essential to ensure reliable operation.

4. Sheet Fixture

The momentum probe was used to evaluate the characteristics of an axially symmetric liquid sheet formed by an annular slit flow fixture, also described in Ref. 12. The 0.018-in.-wide sharp-edged slit was formed by the juxtaposition of two identical orifice assemblies as shown in Fig. 7. Each assembly consisted of a 1-in.-D barrel

supplied from an upstream system designed to minimize flow disturbances. After passing through a 200-mesh screen, the flow executed a 90-deg turn through a vaned elbow. While a very long, straight approach section would have been ideal for achieving the quiescent, laminar flow desired, space limitations made the use of the elbows necessary. Six vanes were inserted in each elbow in an attempt to preserve the velocity profile existing upstream of the turn. Following the elbow were three 200-mesh screens spaced 1.5 (D) apart, with an 8-L/D plenum chamber immediately upstream of the exit.

This flow system was built in an effort to simulate the flow conditions which exist in a sheet formed by the impingement of two opposed, identical, *laminar*, liquid jets having *uniform* velocity profiles. Such a sheet is of interest because it represents a relatively stable flow geometry; moreover, it bears a close resemblance to the electrical analog solution of the potential flow of a jet impinging upon a flat plate studied by Le Clerc (Ref. 13). This similarity should prove useful in evaluating the data obtained from such a sheet. The sheet fixture was built in order to circumvent an intrinsic problem of spatial stability of the impingement point which results when liquid jets having the hydrodynamic properties described above are used to form a free sheet. It should be noted that a stable impingement-point location is established

where the centerline stagnation pressures of the two impinging jets are equal (Ref. 12). In the case of a free, *laminar, uniform* velocity profile jet, the centerline stagnation pressure is constant everywhere. Hence, for two identical jets of this type, a neutrally stable impingement location can be established at any point along their free length. However, since no restorative force is present, a slight, inadvertent perturbation in the flow rate of either jet, for instance, would cause a corresponding change at the impingement point, thus resulting in a nonreproducible sheet location. The sheet fixture produces a free sheet which retains the stable characteristics of the laminar sheet formed by an impinging jet arrangement, while eliminating the unstable-impingement-point problem associated with such a scheme.

C. Calibration and Instrumentation

In order to measure the thrust produced by the flow impinging on the momentum probe, the electrical output of the secondary beam, which serves as the force measuring element in the system, must be related to the deflection at its free end. When the probe is in use, the deflection results from the force applied to the secondary beam via the pivot pin system from the deflection plate and the attached primary beam. The calibration was accomplished by loading the beam while in
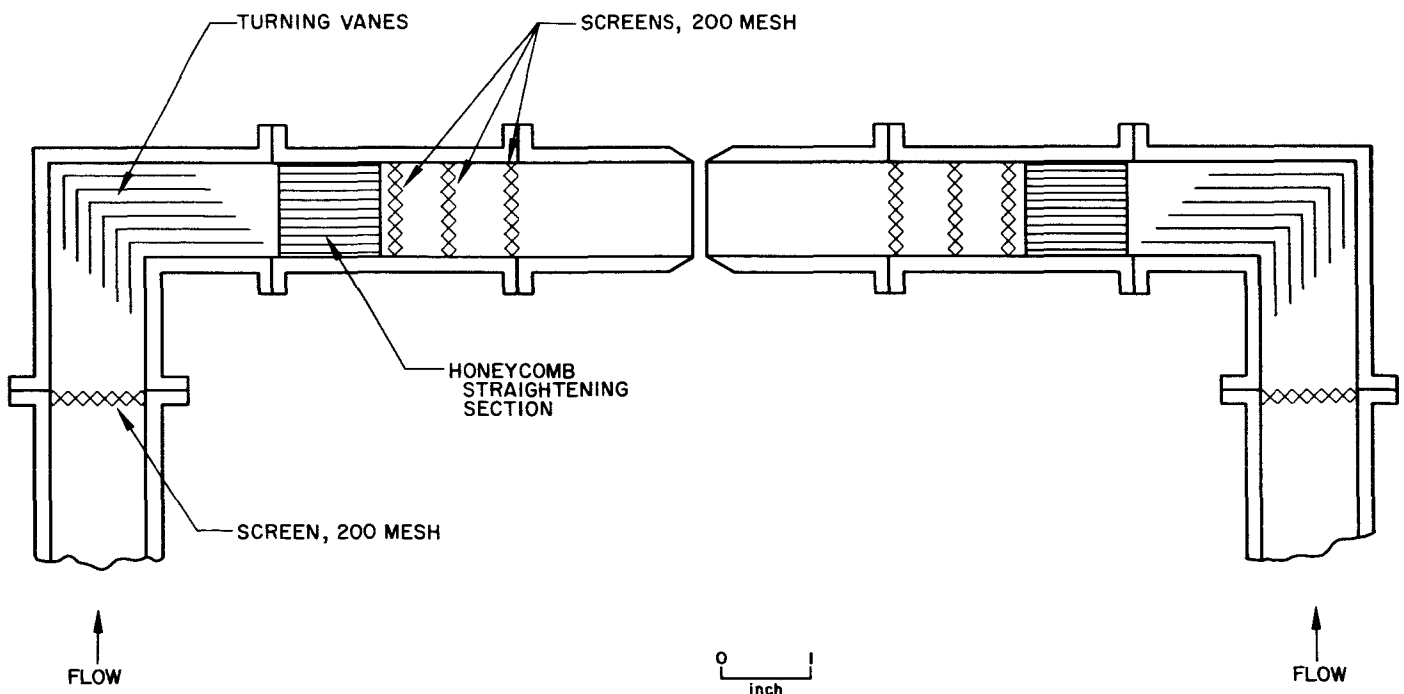

Fig. 7. Details of sheet fixture

a horizontal position with dead weights hung at the point through which the force vector acted when the apparatus was assembled. Throughout each beam's usable range (see listing in Fig. 5), the strain-gage-bridge output vs. the applied load was very nearly linear.

Accurate initial alignment of the deflectors was required, since each probe was designed to operate properly at only one specific radial location. Seven alignment discs were fabricated which had the same radii as the deflection plates. Each disc was made in two halves which were fitted closely around the barrel assemblies on the spray fixture, so that the periphery of the positioned disc served as the reference surface. The appropriately sized probe was adjusted until it conformed to the position of the reference surface and the strain-gage-

bridge output of the primary beam was noted. The disc was then removed, leaving the deflector still in place. Deviations from the established location of the probe could then be detected simply by monitoring the electrical output of the primary beam.

The Baldwin Model C-12-141 strain gages used to instrument the beams were electrically excited by Microdot Model PB-90 DC power supplies. The outputs of the strain-gage bridges were recorded on Speedomax analog recorders. The flow rate was measured with a Waugh Model FL8-S turbine flow meter connected to a Hewlett–Packard EPUT counter. The test fluid was water, and suitable density corrections for temperature were applied. The work was performed at JPL's Atomization Laboratory.

III. EXPERIMENTAL RESULTS

A. Presentation of Data

The data generated in a typical run using the momentum probe consisted of a thrust reading and a weight flow measurement. As discussed in Section I-D, this information is sufficient to permit both the average local velocity of the sheet and the local sheet thickness to be computed. As was shown, the average velocity of the sheet at the point where the measurement was made is given by

$$V = \frac{2\pi F g}{\dot{w}}$$

In addition, the local momentum averaged sheet thickness can be expressed as

$$t = \frac{\dot{w}^2}{4\pi^2 r \rho F g}$$

The results obtained when these relations were applied to the experimental data are presented in Fig. 8,

where the momentum averaged thickness of the sheet is plotted vs. the average sheet velocity for the several radial locations studied. These data were then cross-plotted to produce the curves presented in Fig. 9, which show the variation of sheet thickness with the sheet radius at several representative sheet velocities.

B. Discussion of Results

The variation in sheet thickness occurring as a function of sheet velocity is shown in Fig. 8. The lowest velocity that could be evaluated corresponds to the condition of initial breakaway of the sheet from the edge of the deflector plate. Because of surface tension effects, the liquid would not separate cleanly from the plate at very low flow velocities. Above the minimum velocity indicated in the Figure ($\sim$ 21 ft/sec), however, the separation of the flow from the plate was well defined. As mentioned in Section II-B1, measurements made of the angle at which the sheet left the surface of the deflector indicated that no appreciable deviation in the assumed 90-deg turning angle occurred as the flow velocity exceeded this minimum value.
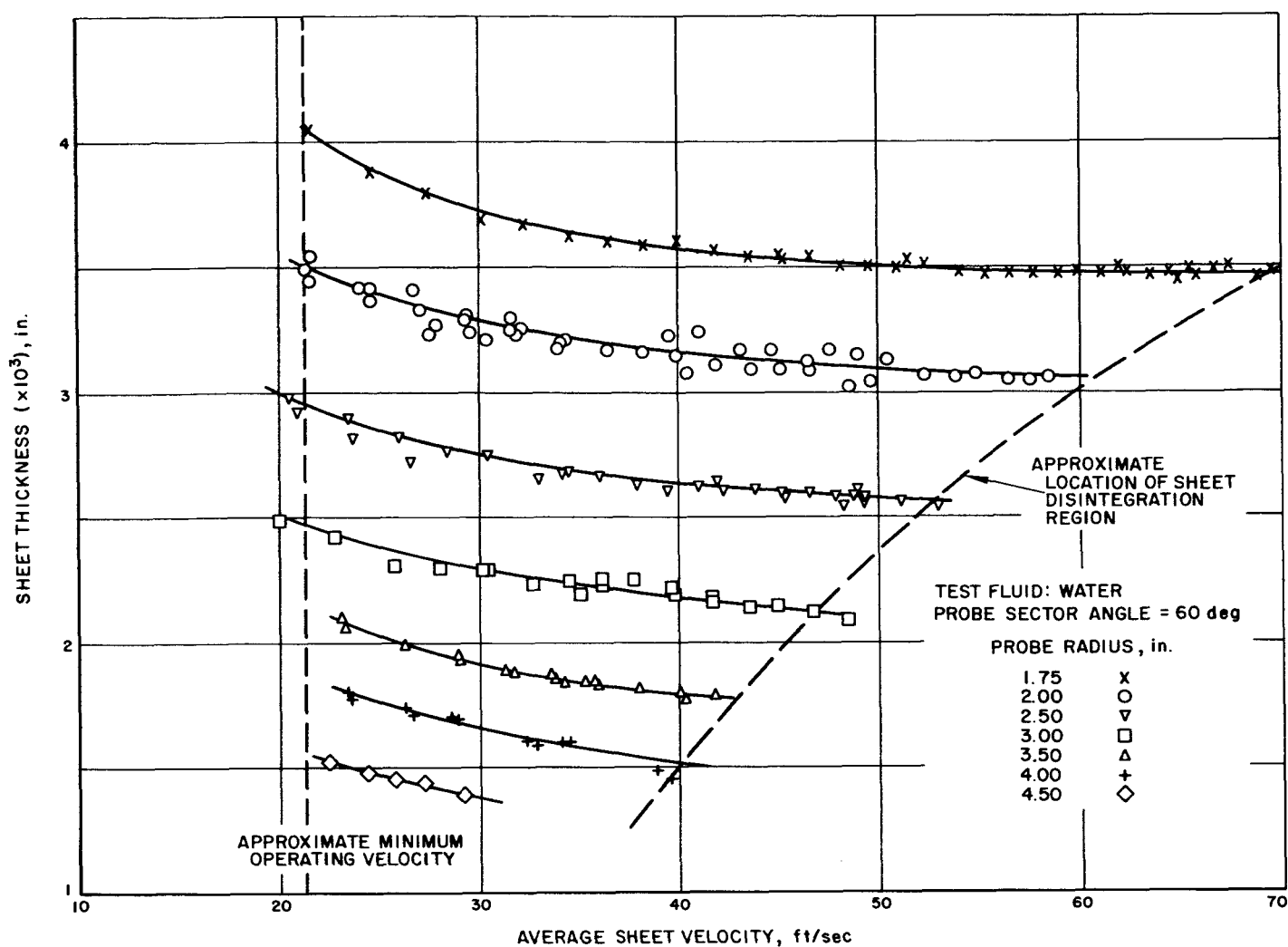
Fig. 8. Sheet thickness vs. sheet velocity at various radii

The limit on the highest sheet velocity that could be evaluated using the momentum probe was imposed by the experimental difficulties caused by the sheet disintegration zone nearing the deflection plate. As the velocity of the sheet was increased, the radius at which sheet breakup occurred decreased, thus moving the breakup zone closer to the fixed location of the probe. As it did so, a high-pitched whistling noise became audible, increasing in intensity as the zone approached the plate; at the same time, the output of the secondary beam became more irregular. These perturbations in the records caused some difficulty in reducing the experimental data. Ultimately, the breakup zone reached the probe, resulting in intermittent flow on the plate and erratic thrust readings from the secondary thrust beam. The upper limit on the velocity was established as the point

at which the noise generated by the approach of sheet breakup region to the probe became noticeable. The upper bound on the data resulting from this flow phenomenon is noted in Fig. 8.

Figure 9 illustrates the interrelation of the sheet thickness with radius for several representative average flow velocities. The data can be well represented in each case by a straight line with a slope of −1.0. The maximum deviation observed between a datum point and its respective curve was 3%. Thus, it is seen, for the flow configuration studied and within the limits stated, that the thickness varied inversely with the radius. Note that since $tr = $ constant and $\dot{w} = \rho V 2\pi r t$, then, for a given flow rate, the velocity V is invariant throughout the sheet.
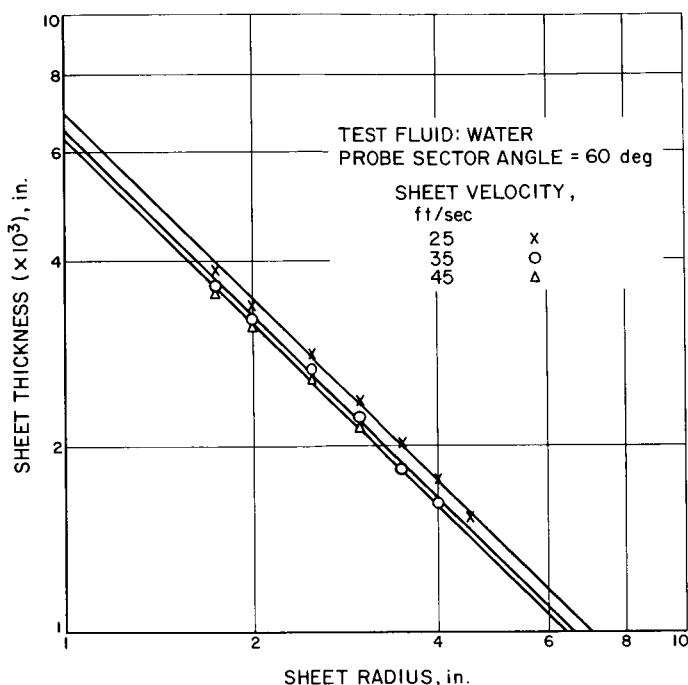
Fig. 9. Sheet thickness vs. sheet radius at various velocities

It is noted from Fig. 9 that the thickness of the sheet at a given location in the flow decreases as the velocity is increased. This effect is probably due to *vena contracta* effects induced by the sharp-edged annular orifice used to produce the sheet. When describing *vena contracta* phenomena, it is conventional to compute a contraction ratio, defined as the minimum-flow cross-sectional area divided by the orifice area. However, in this flow configuration such a calculation has no meaning because the sheet thickness is not constant. Nevertheless, an "effective" contraction ratio may be determined by considering the flow geometry predicted by the empirically determined relation tr = constant. The *apparent* thickness at the annular slit location may be computed by evaluating the constant at some convenient location in the flow. This computation is predicated on the hypothesis that the origin of the flow is a line source of infinite extent located at the axis of symmetry. The ratio of the thickness computed at the location of the slit to the actual width of the slit can be thought of as an "effective" contraction ratio for this particular flow scheme. The values determined in this manner range from 0.778 to 0.706 as the corresponding sheet velocities vary from 25 to 45 ft/sec. It is of incidental interest to note that the theoretical contraction ratio for a two-dimensional jet is $\pi/(\pi + 2)$, ($\sim$0.611). It is important to recognize that such a flow configuration does not model the axially symmetric geometry under consideration here and, hence, results obtained for these two cases are not expected to be similar.

IV. SUMMARY OF RESULTS AND CONCLUSIONS

1. The momentum-balance technique has been shown to be suitable for measuring the thickness and average velocity of certain types of free, thin liquid sheets.

2. It was found, for the sheet configuration studied, that the sheet thickness varied inversely with the radius of the sheet and, hence, the average velocity was constant throughout the flow field. It was fur-

ther noted that "effective" contraction ratios of from 0.706 to 0.778 were determined for the sheet velocity range studied, thus indicating a *vena contracta* effect in the sheet.

3. The method was found to be applicable to the determination of sheet thickness only in the continuous flow regime of the sheet.

14

NOMENCLATURE

F force, lb

g gravitational constant, 32.2. ft/sec^2

r sheet radius measured from flow axis of symmetry, ft

t sheet thickness, ft

T working beam thickness, in.

V average velocity of sheet, ft/sec

$\dot{w}$ total weight flow rate of sheet, lb/sec

ρ liquid density, lb/ft^3

REFERENCES

1. Rupe, J. H., On the Dynamic Characteristics of Free-Liquid Jets and a Partial Correlation With Orifice Geometry, Technical Report No. 32-207, Jet Propulsion Laboratory, Pasadena, California, January 15, 1962.

2. Ranz, W. E., "Some Experiments on the Dynamics of Liquid Films," Journal of Applied Physics, Vol. 30, No. 12, December 1959, pp. 1950–55.

3. Weber, C., "Zum Zerfall eines Flüssigkeitsstrahles," Zeitschrift für angewandte Mathematik und Mechanik, Vol. 2, 1931, pp. 136–154.

4. Jaivin, G. I., "Atomization and Injection," Research Summary 36-14 (February 1, 1962–April 1, 1962), Jet Propulsion Laboratory, Pasadena, California, May 1, 1962, pp. 133–142.

5. Dombrowski, N., and Fraser, R., "A Photographic Investigation into the Disintegration of Liquid Sheets," Philosophical Transactions of the Royal Society, Vol. A247, 1954, p. 101.

6. Dixon, B., Russell, A., and Swallow, J., "Liquid Films Formed by Means of Rotating Discs," British Journal of Applied Physics, Vol. 3, 1952, p. 115.

7. Dombrowski, N., Ward, D., and Hasson, D., The Mechanics of Liquid Flow Through Fan Spray Nozzles, Imperial College Report JRL No. 43, October 1958.

8. Dukler, A., and Bergelin, O., "Characteristics of Flow in Falling Liquid Films," Chemical Engineering Progress, Vol. 48, 1952, p. 557.

9. Berthold, T., Measuring Thickness by Radioactivity, British Patent 692,609, 10/3/52.

10. Wilkes, J., and Nedderman, R., "The Measurement of Velocities in Thin Films of Liquid," Chemical Engineering Science, Vol. 17, 1962, p. 177.

11. Lukens, H., Jr., "Film Thickness Determination with a Scintillation Counter," Analytical Chemistry, Vol. 34, No. 11, October 1962, p. 1396.

12. Jaivin, G. I., "Atomization and Injection Hydraulics," Research Summary 36-4 (June 1, 1960–August 1, 1960), Jet Propulsion Laboratory, Pasadena, California, September 1, 1960, pp. 77–78.

13. LeClerc, A., Deflection of a Liquid Jet by a Perpendicular Boundary, Master's Thesis, Department of Mechanics and Hydraulics, State University of Iowa, Iowa City, 1948.